

Amherst 2 K
April 9 - 12, 2000
University of Massachusetts
Amherst

PREPRINT

Fellenius, B. H., Brusey, W. G., and Pepe, F., 2000. Soil set-up, variable concrete modulus, and residual load for tapered instrumented piles in sand. American Society of Civil Engineers, ASCE, Specialty Conference on Performance Confirmation of Constructed Geotechnical Facilities, University of Massachusetts, Amherst, April 9 - 12, 2000, 16 p.

Soil Set-up, Variable Concrete Modulus, and Residual Load for Tapered Instrumented Piles in Sand

Bengt H. Fellenius¹⁾, Walter G. Brusey²⁾, and Frank Pepe³⁾

ABSTRACT. Two 20 m long, strain-gage instrumented, closed-toe, 350-mm Monotube piles with a 7 m long bottom section tapering down to a 200-mm diameter at the pile toe were driven into a deposit of silty sand of glacial origin. The piles were concreted and static loading tests were performed—one pile was tested three days after completion of driving and concreting and the other after twenty-three days. The static test established the former pile to 2,000 KN. A maximum load of 2,500 KN was applied to the pile tested after twenty-three days without reaching the ultimate resistance of the pile, confirming the experience of earlier tests at the site that the pile capacity increases with time due to set-up. The actual magnitude of the set-up was not established. Both piles were instrumented with vibrating wire strain gages. The measurements showed that the pile Young's modulus of the composite steel concrete was not a constant but a linear function of the imposed strain. The measured axial strains were used to determine the non-constant Young's modulus of the steel-concrete cross section, enabling calculation of the axial loads in the piles during the test. The test data showed that locked-in load (residual load) acted on the piles before the start of the loading tests. The point of equilibrium (neutral plane) between downward and upward acting residual load forces on the pile was determined to be close to where the pile cross section changed from a straight section to a tapered section. Because of the presence of residual load, the measured loads indicated, falsely, that the soil resistance acting against the tapered section pile was very small. The analysis determined the magnitude and distribution of the actual shaft and toe resistances as well as of the residual load proving that most of the pile capacity was developed in the bottom portion of the pile agreeing well with effective stress principles. In the tapered section, at the maximum applied test load, the resistance was governed by fully mobilized positive shaft resistance and a movement-dependent "toe resistance component". The analysis results suggest that the set-up was due to a stiffening of the soil and not to increase of shaft resistance. The following effective stress soil parameters were established for the two test piles, Piles 2 and 3: beta-coefficient equal to 0.4 and N_t -coefficients of 60 and 75, respectively.

¹⁾ Urkkada Technology Ltd., 1010 Polytek St., Unit 6, Ottawa, ON, K1J 9H8

²⁾ The Port Authority of New York and New Jersey, One World Trade Center, New York, NY 10048

³⁾ Parsons, Brinckerhoff, Quade, and Douglas Inc., 1 Penn Plaza, New York, NY 10119

INTRODUCTION

Since the early 1990's, the JFK Airport is seeing extensive rebuilding and upgrading. Due to the particular soil conditions at the airport, structures must be supported on pile foundations. The pile of preference at the airport is the Monotube pile, a thin-wall steel pipe with a 350-mm or 450-mm (14 in or 18 in) diameter connected to a 7.6-m (25 ft) lower section that tapers down to a 200-mm (8 in) diameter at the pile toe. The piles were subject to considerable testing at the start of the construction using static and dynamic testing and analysis methods. York et al. (1995) presented results from static loading tests on piles installed to depths ranging from 16 m through 23 m and performed 15 days through 42 days after driving. The capacities established in the static tests were combined with pile capacities obtained from WEAP analysis and Pile Driving Analyzer tests with CAPWAP analysis on driving records from five piles at initial driving and at restrrike 49 days after driving. The results indicate that the pile capacity increased on average by approximately 50 percent during the first about three weeks after the driving. In 1994, additional testing was undertaken consisting of static loading tests on two instrumented piles. The results of the 1994 tests are presented in the following.

SOIL CONDITIONS

Details on the soil conditions at the site are available in York et al. (1995). In summary, the site is located adjacent to the Jamaica Bay on the south shore of Long Island, New York, and was developed in the 1940's from an existing marsh by placing sand dredged from the bay bottom to about 4 m height at the subject location. The groundwater table lies at 2.5 m below the fill surface and the pore pressure distribution is considered to be hydrostatic. The fill was placed on the original marsh organic material, which has a thickness at the subject location of about 1 m and consists of soft clay and peat. Below the marsh material, the soil consists of fine to coarse, medium dense to dense, glacial sands to large depth. Fig. 1 shows the results of a cone penetrometer test (CPTu) from the test site (the cone stress is q_t , i. e., it has been corrected for pore pressure on the shoulder). The cone profile identifies the original marsh surface at a depth of 4 m to 5 m and shows that the sand is relatively uniform down to 25 m and contains both dense ($q_t > 10$ MPa), compact ($5 \text{ MPa} < q_t < 10$ MPa) layers, as well as, occasionally, loose ($q_t < 5$ MPa) layers. The pore pressure profile indicates that dilating zones exist at 18 m and at 23 m.

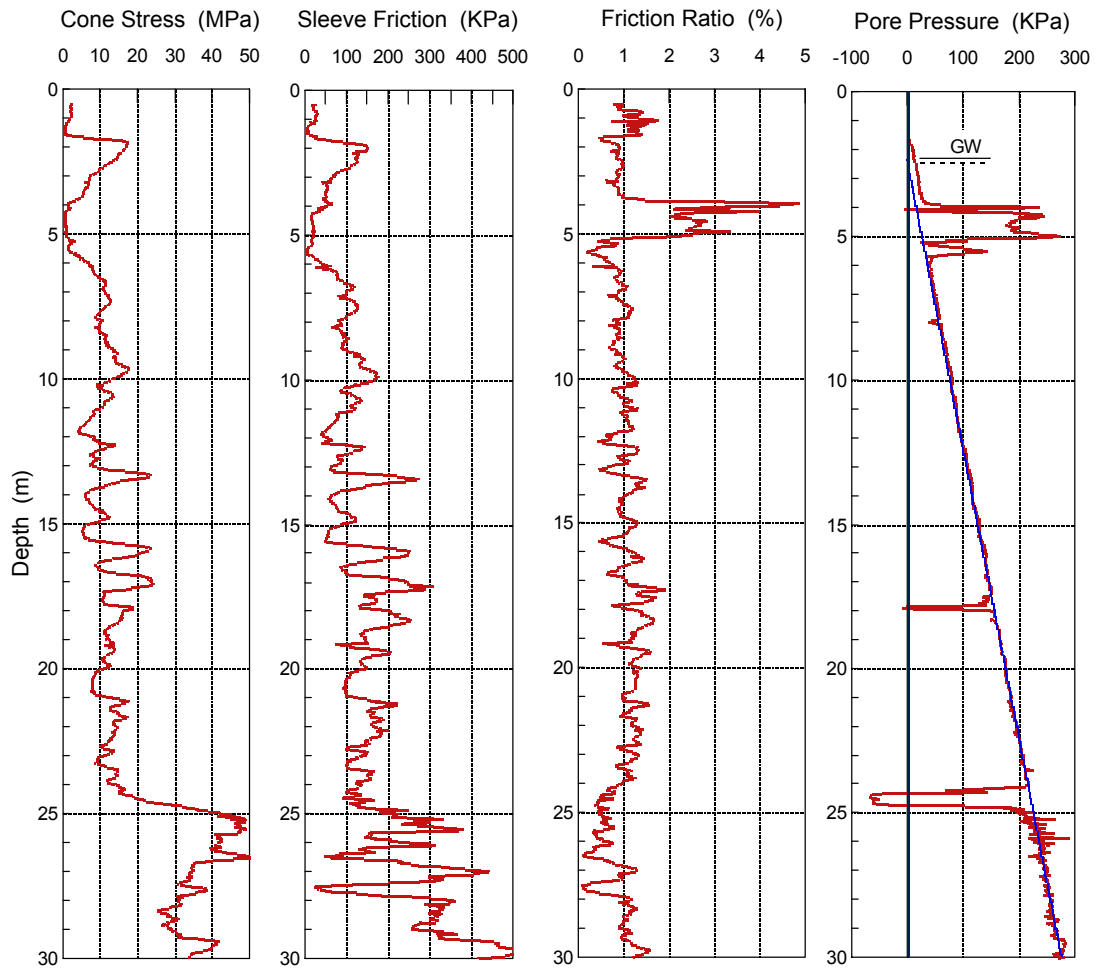


Fig. 1 CPTu Diagram

TEST OBJECTIVES

The objectives of the test are:

1. Confirm the presence of set-up at the site
2. Determine the pile capacity and the load-transfer (the distribution of shaft resistance along the pile and the pile toe resistance)
3. Determine the effect of a linearly variable Young's modulus in the composite (steel and concrete) pile cross section
4. Evaluate the magnitude of residual load

TEST PILES

The test piles, designated Pile 2 and Pile 3, consist of 21 m (70 ft) long, 357 mm (14-in), closed toe Monotube piles with the lower 7.6 m (25 ft) tapered 2.1 percent (0.25 in per foot) to a 203-mm (8-in) toe diameter. The wall thickness was 5.3 mm (0.209 in). The piles were installed by driving about 8 m apart and were filled with a 28 MPa (4,000 psi) concrete immediately after end of driving.

PILE INSTRUMENTATION

The test piles were instrumented with surface-mounted and embedment-mounted vibrating wire strain gages, which were placed at seven depth levels in the piles with two surface-mounted gages and one embedment gage at each level. The distances below the pile head and the depths below the ground surface to the gage levels of are given in Table 1.

The surface-mounted gages, Geokon Model VSM-4000, were attached before installation of the pile at diametrically opposed points and protected by a steel angle welded to the pile. The embedment gage, Geokon Model VSM-4200, was installed after driving, but before concreting, in a 25 mm (1.0 in) diameter pipe with a 3.2 mm (0.125 in) thick wall positioned at the center of the pile. A Geokon GK data-logger and read-out unit was used to record all gage data during the static loading tests.

Gage Level 1 was placed above the ground to serve as reference for determining the elastic modulus of the composite pile, steel and concrete, necessary for converting the strain to stress in the pile.

PILE INSTALLATION

The piles were driven with a Vulcan 010 hammer having a rated energy of 44 KJ (32.5 ft-kips). The penetration resistance at the end of driving was 35 blows/0.3 m for both piles.

Pile 2 met an obstruction at the depth of the original ground surface, later found to be three chunks of concrete. After several attempts to drive through the obstruction, the pile was withdrawn and the obstructions were dug up. The “hole” was then backfilled without compaction and the pile driving was resumed in the same location. In the process, the pile became slightly bent, misaligned by about 3 degrees, and the pile head was curled. As a consequence, some of the strain gages in Pile 2 did not survive the installation and other gages on the pile gave erratic values during the loading test.

TABLE 1 Gage locations in Pile 2 and 3

Gage Level	Pile 2		Pile 3	
	Distance Below Pile Head (m)	Depth Below Ground (m)	Distance Below Pile Head (m)	Depth Below Ground (m)
1	0.5	--	0.7	--
Ground surface	1.0	0	0.5	0
2	2.6	1.6	3.0	2.3
3	4.7	3.7	4.9	4.4
4	9.0	8.0	9.2	8.7
5	12.7	11.8	12.9	12.4
Start of taper	13.4	12.4	13.7	12.9
6	16.9	15.9	17.1	16.6
7	20.3	19.3	20.5	20.0
Pile toe	20.9	20.0	21.3	20.5

STATIC LOADING TEST

The loading tests was by Maintained-Load method with about 62 KN (14 kips) load increments, which were applied at intervals ranging from 6 minutes to 18 minutes. Loads were obtained by jacking against a loaded platform. The loads were applied by a single jack and determined by a separate load cell. Records were obtained by means of the data logger set to scan the gages at 3-minute intervals.

Static axial compression tests were performed three days (Pile 2) and twenty-one days (Pile 3) after the end of driving. Pile 2 was unloaded at the maximum load of 2,200 KN (225 tons), occurring at a movement of 18 mm (0.7 inch) when the load-movement curve reached the offset limit load (Davisson, 1972). Pile 3 was unloaded when the applied load reached 2,500 KN (280 tons), the maximum capacity of the reaction system.

RESULTS AND DATA REDUCTION

Load-Movement Curves

Fig. 2 presents the load-movement curves from the two static loading tests. The two diagrams have been supplemented with the elastic line (marked AE/L) drawn from the Davisson offset limit load.

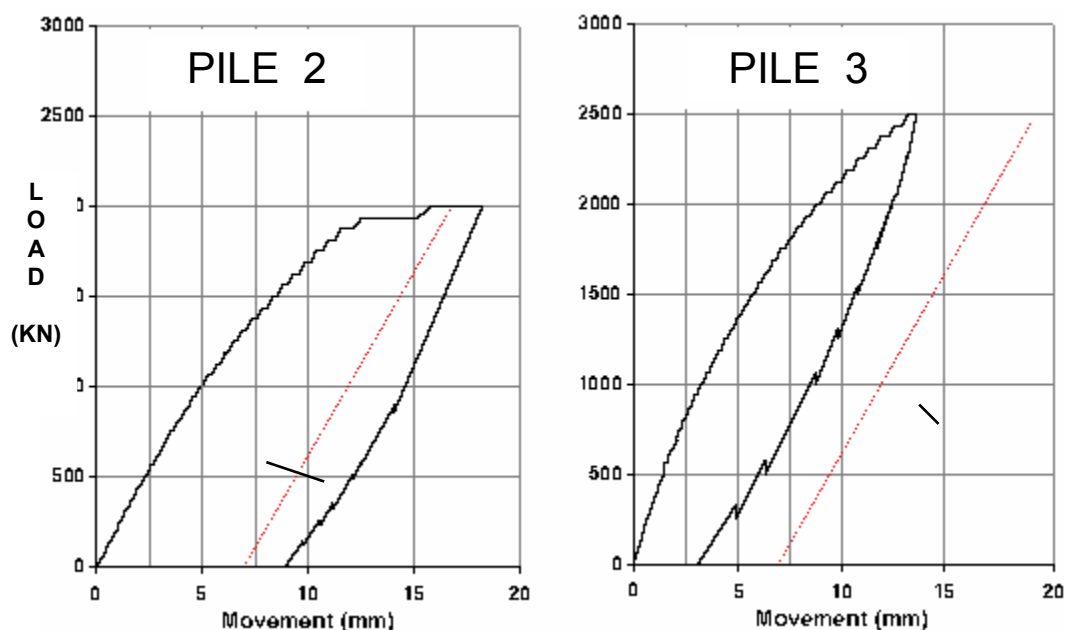


Fig. 2 Pile Head Load-Movement Curves. Piles 2 and 3

Pile 2 demonstrates a less stiff response to the loading than does Pile 3. The ultimate resistance was reached for Pile 2 at the applied load of 2,000 KN, as indicated by the offset elastic line intersecting the load-movement curve. In contrast, no offset-limit intersection occurred for the Pile 3 test curve, which means that the ultimate resistance exceeds the maximum test load of 2,500 KN (280 tons).

The soil conditions and the two test piles are in all respects equal. Therefore, the results of the static tests showing that maximum test load applied to Pile 3 is 25 percent larger than the capacity of Pile 2 indicates that the previously noticed (York et al., 1995) presence of set-up of the sand at the site is valid.

The observed setup is not due to dissipation of pore pressures induced during the driving of the piles (change of effective stress). In the sand at the site, pore pressures induced during the driving dissipate very quickly after the last blow.

Strain Measurements and Elastic Modulus

As mentioned, the initial difficulties in driving Pile 2 resulted in the loss of several of the surface-mounted strain-gages. Also, a few of the surface-mounted strain-gages in Pile 2 did not survive the continued pile driving, which was evidenced by their very erratic reading values. Moreover, while the surface-mounted gages in Pile 3 show readings of similar value, the gages in Pile 2 show differences indicating bending. During both tests, electronic noise affected many individual gage values.

Many of the same-scanning-event gage readings were recorded before, during, or immediately after a load increment was applied to the pile head. Therefore, the time log was carefully reviewed and each reading was placed with its proper load. Readings taken when the load increment was being applied were discarded. In Pile 2, bending caused some gage readings to become obviously erroneous, and these were also discarded as were the values affected by electronic noise.

Only a few of the records from Pile 3 had to be discarded. Fortunately, a large number of readings were taken and this redundancy ensured that reasonably reliable records are available from every load applied to the pile head and from every gage level. However, the accuracy of the Pile 2 test data is lower than that of the Pile 3 data.

Fig. 3 presents a diagram of the applied load versus measured strain. For Pile 2, the strain readings at Levels 1, 2, and 3 are almost identical, whereas the readings at these levels differ for Pile 3. This is due to that only little shaft resistance developed along Pile 2 in the loose backfill.

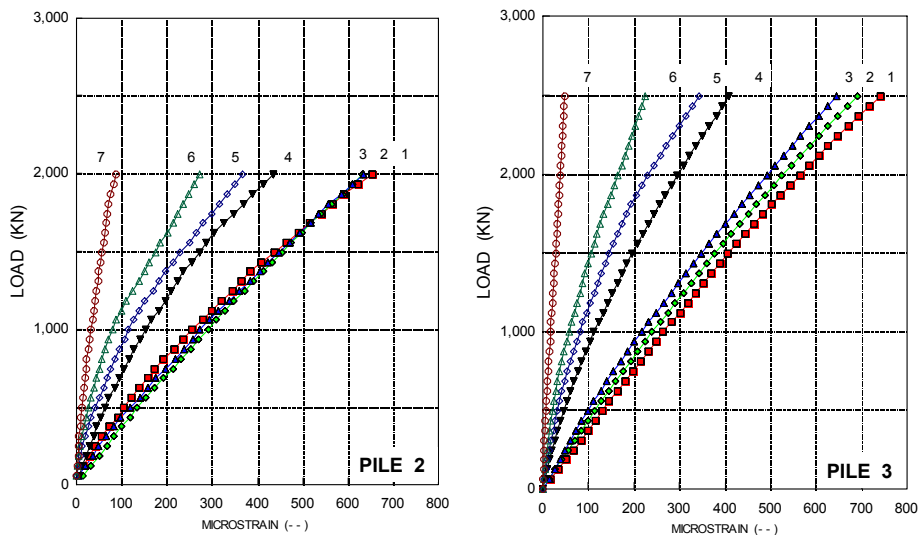


Fig. 3 Strain measured at each gage level. Piles 2 and 3

In contrast to the elastic modulus of steel, the elastic modulus of concrete is not a constant, but a function of the imposed strain. Over the large stress range imposed during a static loading test on a concreted pipe pile, the difference can be substantial between the initial and the final moduli for the composite steel and concrete material. Fellenius (1989) presented a method for the evaluation of the modulus from the actual test data and showed that:

1. For a pile taken as a free-standing column (case of no shaft resistance), the tangent modulus of the composite material is a straight line sloping from a larger modulus value to a smaller.
2. Every measured strain value can be converted to stress by its corresponding strain-dependent secant modulus.

The Fellenius (1989) method for the evaluation is summarized in the following.

The equation for the tangent modulus line is:

$$(1) \quad M = \frac{d\sigma}{d\varepsilon} = A \varepsilon + B$$

which can be integrated to:

$$(2) \quad \sigma = A \varepsilon^2 + B\varepsilon$$

However,

$$(3) \quad \sigma = E_s \varepsilon$$

Therefore,

$$(4) \quad E_s = 0.5 A \varepsilon + B$$

where $M =$ tangent modulus

$E_s =$ secant modulus

$\sigma =$ stress

$d\sigma = (\sigma_{n+1} - \sigma_1) =$ change of stress from one reading to the next

$A =$ slope of the tangent modulus line

$\varepsilon =$ measured strain

$d\varepsilon = (\varepsilon_{n+1} - \varepsilon_1) =$ change of strain from one reading to the next

$B =$ y-intercept of the tangent modulus line (i.e., initial tangent modulus)

With knowledge of the strain-dependent secant modulus relation, the measured strain values are converted to the stress in the pile at the gage location. The load at the gage is then obtained by multiplying the stress with the pile cross sectional area.

When data reduction is completed, the evaluation of the test data starts by plotting the tangent modulus, that is, for each load increment, values of change of stress over change of strain are plotted versus measured strain. For a gage located near the pile head (in particular, if above the ground surface, e. g., for Gage Location 1 in the two test piles), the modulus calculated for each increment is unaffected by shaft resistance and the calculated tangent modulus is the actual modulus. For gages located further down the pile, the first load increments are substantially reduced by shaft resistance along the pile above the gage location and, therefore, the load change at the gage is smaller than the applied increment of load. Consequently, the modulus values calculated from the first load increments are large. However, as the shaft resistance is being mobilized down the pile, the calculated modulus values become smaller. When all shaft resistance above a gage location is mobilized, the calculated values are the tangent moduli for that gage location.

Presence of shaft resistance above a gage will make the tangent modulus line plot below the modulus line for an equivalent free-standing column. The larger the shaft resistance, the lower the line. However, the slope of the line is unaffected by the amount of shaft resistance above the gage location. The lowering of the line is not normally significant. However, it is a good rule to determine the tangent modulus line by placing one or two gages near the pile head where the strain is unaffected by shaft resistance. An additional reason for having a reference gage level with or even above the ground surface is that such a placement will also eliminate any influence from strain-softening of the shaft resistance. If the shaft resistance exhibits a strain-softening, the calculated modulus values will become smaller, and infer a steeper slope than the true slope of the modulus line. If the softening is not gradual, but suddenly reducing to a more or less constant post-peak value, a spike will appear in the diagram.

Fig. 4 presents the tangent modulus plots for the test piles. The upper diagram pair includes the data from all gage levels with the modulus axis in logarithmic scale (in order to fit all values into the diagram). The lower pair shows the modulus values in a linear scale for the four uppermost gage levels (those in the straight portion of the test piles). The values from the gage levels located in tapered portion of the piles (Levels 5 through 7) are too large to fit into the linear-scale diagram.

Fig. 4 shows that tangent modulus values for the four uppermost gages, Gages 1 through 5, converge to a straight line. The line represents the tangent modulus of the equivalent column representative for a pile unaffected by shaft resistance. The larger resolution lower diagram shows that the tangent modulus line is immediately established for Gage Level 1, very early for Gage Levels 2 and 3, and somewhat later for Gage Level 4.

Pile 2

Pile 3

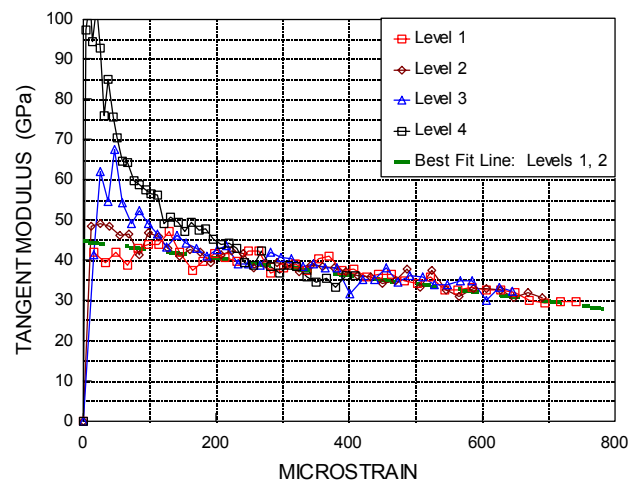
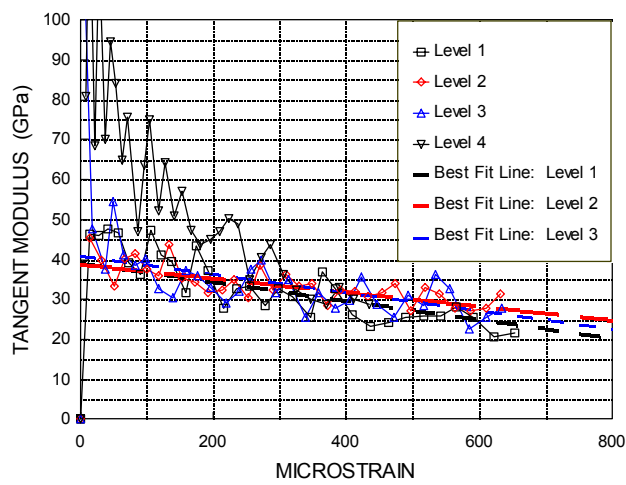
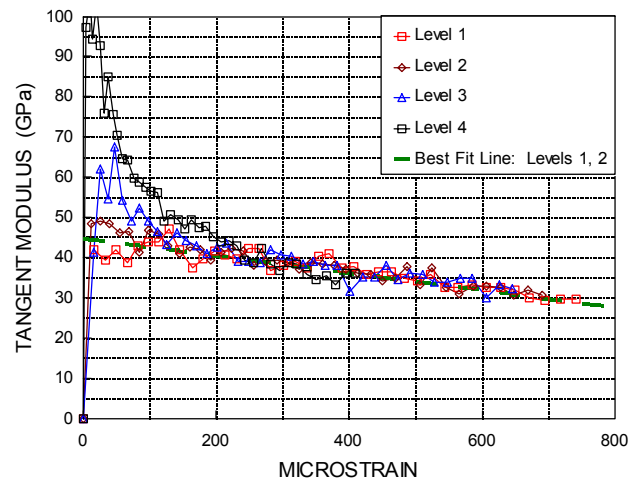
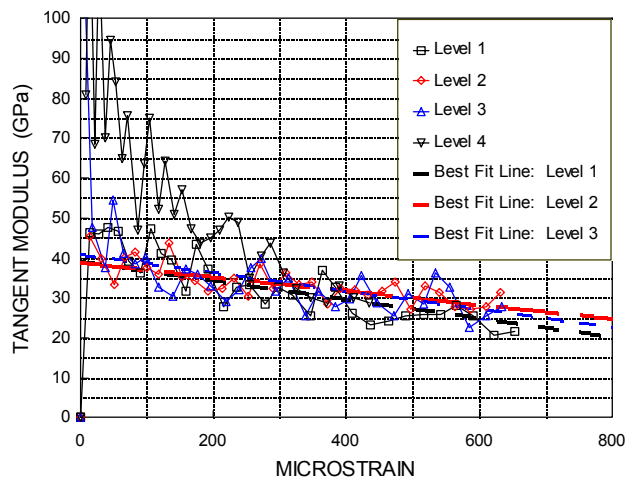
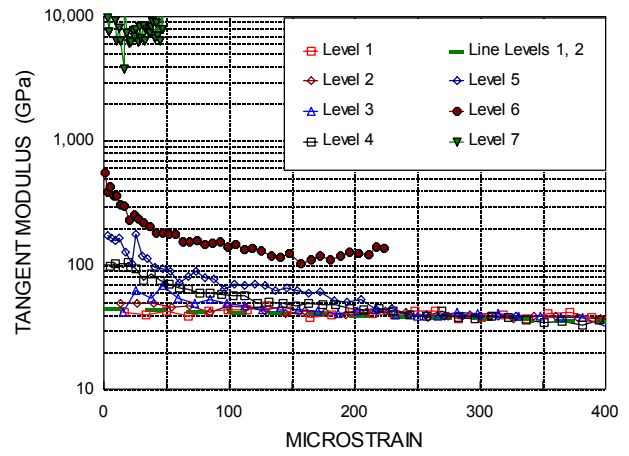
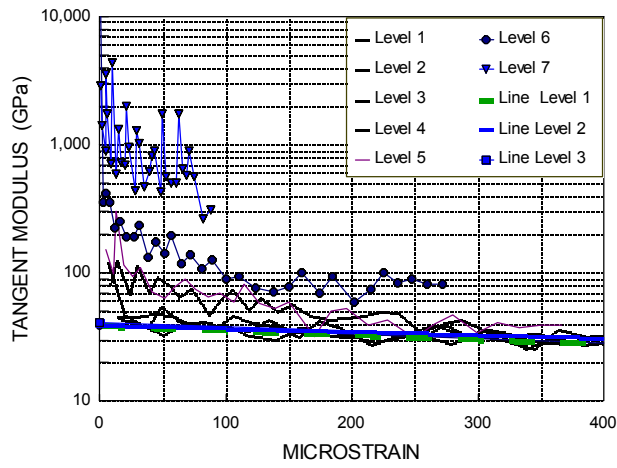


Fig. 4 Tangent modulus diagram. Piles 2 and 3

In contrast to the higher up gage levels, Gage Levels 6 and 7 do not show modulus values that converge to a modulus line. Even at the end of the test, the tangent modulus values are much larger than those for the straight portion of the piles. It is obvious, therefore, that the actual incremental increase of load at the Levels 6 and 7 is always much smaller than the load increment applied to the pile head. This indicates that the resistance along tapered portion of the piles continues to increase with increasing load. This observation will be addressed later in this paper.

Linear regression of the slope of the Pile 3 tangent-modulus line indicates that the initial tangent modulus is 44.8 GPa (the constant “B” in Eqs. 1 through 4). The slope of the line (coefficient “A” in Eqs. 1 through 4) is -0.021 GPa per microstrain ($\mu \epsilon$). The resulting secant moduli are 42.7 GPa, 40.5 GPa, 38.4 GPa, and 36.2 GPa at strain values of 200 $\mu \epsilon$, 400 $\mu \epsilon$, 600 $\mu \epsilon$, and 800 $\mu \epsilon$, respectively. The Pile 2 strain values do not have the same accuracy, as mentioned, and the diagram shows that the three upper levels indicate slightly different tangent modulus lines. The average of the three lines indicates an initial tangent modulus of 40 GPa and the average slope of the line is about the same as found for Pile 3. The approximately 10 percent difference in modulus between Piles 2 and 3 is consistent with the fact that the concrete had cured for only three days at the time of Pile 2 static test as opposed to 21 days for the Pile 3 test.

The following illustrates the importance of establishing the strain dependency of the modulus: At the applied load of 2,400 KN, Pile 3 Gage Level 3 located at a depth of 4.9 m registered a strain of 625 $\mu \epsilon$. At the same load, Gage Level 5 at a depth of 12.1 m registered a strain of 217 $\mu \epsilon$. The strain values correspond to stress levels of 21.9 MPa and 9.6 MPa, respectively. If the 36 GPa average constant modulus had been used, the stress levels would have become 22.5 MPa and 7.8 MPa. That is, the shaft resistance acting between the two levels would have been determined with an about 10 percent to 20 percent error.

The modulus values for the composite section at Gage Levels 1 through 3 (Pile 2) and Gage Levels 1 and 2 (Pile 3) were correlated to the amount of concrete and steel in the pile in order to determine the concrete moduli. The latter moduli were then used in combination with the steel modulus and the slightly different steel area and concrete areas at Gage Levels 6 through 7 in the tapered section to determine the proportional modulus relation for these gage levels.

Load Distribution

The evaluated coefficient “A” and constant “B” are combined in Eq. 4 to determine the secant modulus relation. The relation is used with the strain data to calculate the stress and load at each gage for each load applied to the pile head.

Fig 5 shows the strain gage readings transferred to load and plotted against depth to give the load distribution in Piles 2 and 3 as evaluated from the measurements during the static loading test.

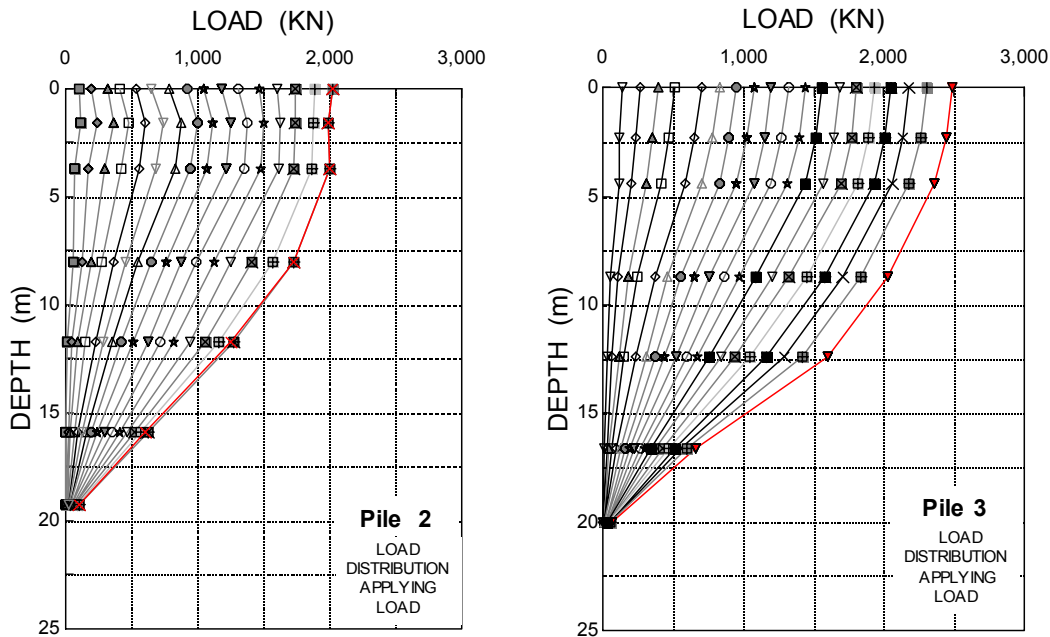


Fig. 5 Load distribution for each load applied to the pile head. Piles 2 and 3

Along the straight shaft portion of the two piles, the calculated distributions of load in the pile are almost identical. This is demonstrated in Fig. 6, where the load distribution curve of Pile 2 showing the values for the gages in the straight portion of the pile has been shifted over (translated) to Pile 3. This means that no set-up of shaft resistance developed along the straight length of the piles .

In contrast, the evaluated distributions within the tapered portion differ for the piles. For Pile 2, the resistance is smaller as indicated by its steeper load distribution curve. Obviously, the 25 percent larger resistance shown for Pile 3 as opposed to the capacity of Pile 2 is obtained along the tapered length of the pile. This means that the increase of capacity (set-up) determined for the time period of three through twenty-three days is not due to increase of shaft resistance expressed by means of the beta coefficient. Instead, the results indicate that the set-up occurred along the taper section and as a consequence of increased soil stiffness during the three-week wait between the two static loading tests, expressed by means of the toe bearing coefficient.

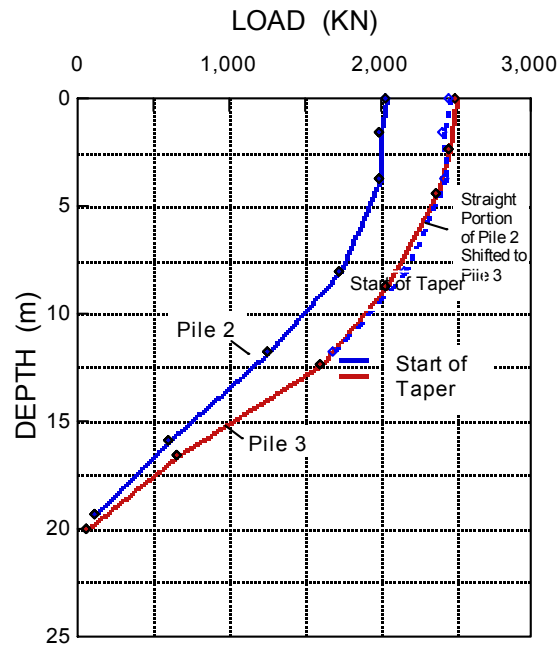


Fig. 6 Load distribution. Comparison between Piles 2 and 3

Residual Load and Soil Parameters

The measured load distributions are not the true load distributions in the piles, as the piles are subjected to residual load. The residual load is generated by fully mobilized negative skin friction along an upper portion of the pile in equilibrium with positive shaft resistance along a lower portion and toe resistance. For the two test piles, the point of equilibrium—the neutral plane—appears to be located shortly below the bottom of the straight portion of the pile, i. e., within the tapered portion of the pile.

Where a straight-shaft pile is subjected to residual load, above the neutral plane, the true load distribution is located at half the distance to the vertical through the pile head load, and is easily constructed (e. g., Altaee et al., 1992). However, below the neutral plane and in a tapered portion, no similarly easy construction is possible. Here, the true load distribution was determined in a series of trial and error using static analysis based on effective stress principles. The analysis was performed using the UniPile program (Fellenius and Goudreault, 1997; details are available on Internet address www.unisoftltd.com).

First, the true shaft resistance along the straight shaft portion of the piles down to Gage Level 5 was determined and employed in a back analysis using effective

stress to determine the beta coefficients, which gave β equal to 0.40—same for both piles.

The conical shape makes the effective stress analysis less direct. It conceivably increases the resistance along the pile shaft as opposed to straight piles. Nordlund (1963) suggested a taper modification factor to use to increase the unit shaft resistance in sand for conical piles. The Nordlund correction factor is a function of the taper angle and the soil friction angle. The taper angle of 1° (0.25-inch/foot) of the subject piles in a sand with a 33° to 37° friction angle would give a Nordlund correction factor ranging from about 2 through about 5.

Fellenius (1996) proposed to use a more direct calculation method consisting of dividing up the soil into sub-layers of some thickness and at the bottom of each such sub-layer project the donut-shaped diameter change. The projected area is treated as an extra pile toe, which analysis is similar to the analysis of a step-taper pile. The shaft resistance is calculated using the mean diameter of the pile over the same “stepped” length. The shaft resistance over each such particular length consists of the sum of the shaft resistance and the extra-toe resistance.

In the continued back-analysis of the test results, the beta-coefficient established for the sand above gage level 5 was assumed applicable also to the soil along the tapered portion of the piles. The assumption is valid considering the uniformity with depth of the soil at the site evident in the CPTu diagram (Fig. 1) and the observation that no set-up developed along the straight length of the piles.

At Gage Levels 5, 6, and 7, the analysis is controlled by the condition that the measured loads are equal to the calculated values of residual load minus the calculated values of true loads. This leaves the analysis of the full length pile with only the toe bearing coefficient, N_t , unknown (applicable to the donut projection of the taper). Calculations were made at every 0.3 m length of the pile and resulted in the following soil parameters for the two test piles: beta-coefficient equal to 0.4 and N_t -coefficients of 60 and 75 for Piles 2 and 3, respectively.

The results of the analysis is presented in Fig. 7 for both Piles 2 and 3, showing the measured and true load distributions, and the difference between these, which is the residual load acting on the pile at the start of the static loading test. The distributions shown are for the maximum test load applied to the piles, which for Pile 2 is the pile capacity defined by the offset limit.

The strain measurements do not include strain caused by the residual load. However, the ‘residual strain’ could be added and a new modulus line be determined. This refinement would have negligible effect on the modulus line determined from Gage Levels 1 through 3 used for determining the tangent and secant moduli. At Gage Levels 4 and 5, the strain due to residual load is small in relation to the strain measured at the end of the test, which means that the residual

load has negligible effect. In contrast, in the middle of the tapered length, Gage Levels 6, the load determined from the strain measured at the end of the test and the calculated residual load before the start of the test are about equal. At the load of 2,500 kN applied to Pile 3, for example, the measured strain is 224 microstrain resulting in a “measured load” of 656 kN. Considering that the measured strain developed when the pile was preloaded by the residual load and that the secant modulus decreases with the strain, the “measured load” is overestimated. On the assumption that the residual strain is equal to the measured strain, 224 microstrain would result in a measured load reduced to 620 kN. Applying this value to the analysis results in a 10 kN to 15 kN reduction in the true load and a similar increase in the residual load with respect to the first determined values. One could go through a few additional loops of calculation toward the end results of a slightly smaller measured load, a slightly larger residual load and a moderately affected true load. However, the precision gained would not warrant the substantial effort required to correct for the residual load.

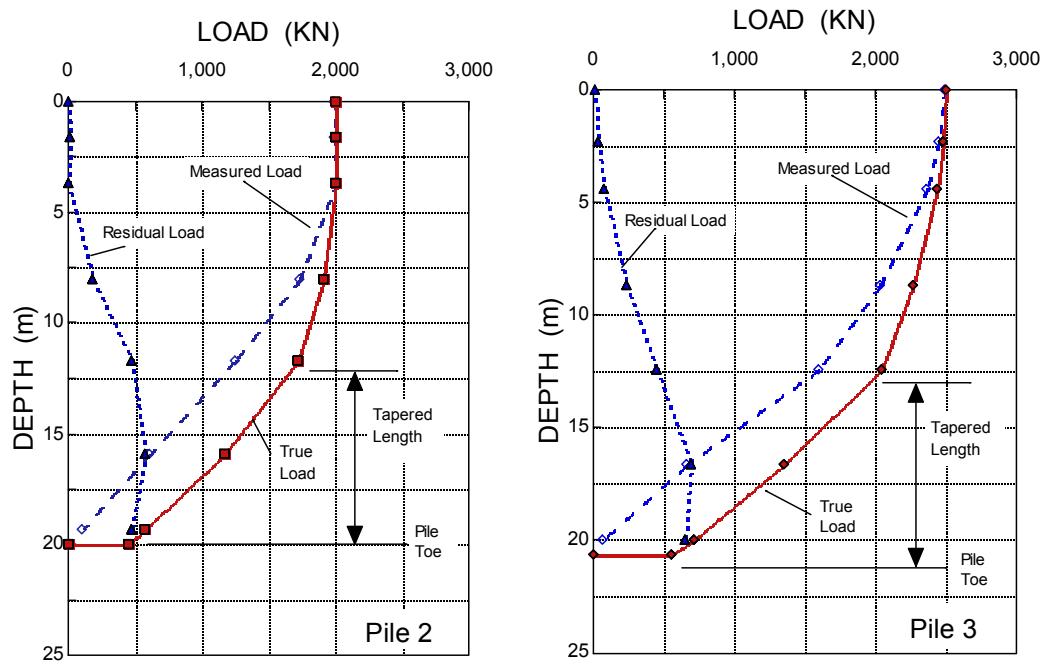


Fig. 7 Distribution of measured load, true load, and residual load. Piles 2 and 3.

CONCLUSIONS

The maximum load applied to Pile 3, tested twenty-three days after installation was 25 percent larger than the capacity of Pile 2 tested after three days. This confirms the experience of earlier tests at the site that the pile capacity increases over time due to set-up. Because the maximum load applied was smaller than the ultimate resistance, the actual magnitude of the set-up was not established.

Because all driving-induced pore pressures have dissipated before the static loading test on Pile 2, the observed set-up is not due to change of effective stress.

The measured strains were used to calculate the tangent and secant moduli for the steel-concrete cross section, enabling calculation of the loads in the piles during the test—the measured loads.

The point of equilibrium (neutral plane) between downward and upward acting residual load forces on the pile was determined to be close to where the pile cross section changed from a straight section to a tapered section.

Because of the presence of residual load, the measured loads indicated, falsely, that the soil resistance acting against the tapered section of the piles was very small. The analysis determined the magnitude and distribution of the actual shaft and toe resistances as well as of the residual load proving that most of the pile capacity was developed in the bottom portion of the pile agreeing well with effective stress principles. In the tapered section, at the maximum applied test load, the resistance was governed by fully mobilized positive shaft resistance and a movement-dependent “toe resistance component”. The analysis results suggest that the set-up was due to a stiffening of the soil and not to increase of shaft resistance.

The following effective stress soil parameters were established for the two test piles: beta-coefficient equal to 0.4 and N_t -coefficients of 60 and 75 for Piles 2 and 3, respectively. Note, the N_t -coefficients represent the resistance mobilized at the respective toe movements.

APPENDIX I — REFERENCES

- Altaee, A., Fellenius, B. H., and Evgin, E., 1992. Axial load transfer for piles in sand. I: Tests on an instrumented precast pile. *Canadian Geotechnical Journal*, Vol. 29, No. 1, pp. 11 - 20.
- Davisson, M. T., 1972. High capacity piles. *Proceedings of Lecture Series on Innovations in Foundation Construction*, American Society of Civil Engineers, ASCE, Illinois Section, Chicago, March 22, pp. 81 - 112.
- Fellenius, B. H., 1989. Tangent modulus of piles determined from strain data. *The American Society of Civil Engineers, ASCE, Geotechnical Engineering Division, 1989 Foundation Congress*, Edited by F. H. Kulhawy, Vol. 1, pp. 500 - 510.

- Fellenius, B. H., 1996. Basics of foundation design. BiTech Publishers, Richmond, BC, 134 p.
- Fellenius, B. H. and Goudreault, P. A., 1997. UniPile Version 3.0 for Windows, User Manual, Unisoft Ltd., Ottawa, 64 p.
- Nordlund, R. L., 1963. Bearing capacity of piles in cohesionless soils. American Society of Civil Engineers, ASCE, Journal of Soil Mechanics and Foundation Engineering, Vol. 89, SM3, pp. 1 - 35.
- York, D. L., Brusey, W. G., Clemente, F. M., and Law, S. K., 1995. Set-up and relaxation in glacial sand. American Society of Civil Engineers, ASCE Journal of Geotechnical Engineering, Vol. 120, No. 9, pp. 1498 - 1513.

APPENDIX II — SYMBOLS USED

M = tangent modulus

E_s = secant modulus

σ = stress

$d\sigma$ = $(\sigma_{n+1} - \sigma_1)$ = change of stress from one reading to the next

A = slope of the tangent modulus line

ε = measured strain

$d\varepsilon$ = $(\varepsilon_{n+1} - \varepsilon_1)$ = change of strain from one reading to the next

B = y-intercept of the tangent modulus line (i.e., initial tangent modulus)

